Thermal Shock Problems of Transversely Isotropic Cylinders with Cracks

Naotake NODA
Shizuoka Univeristy, Hamamatsu, Japan
Fumihiro ASHIDA
Tsuyama National College of Technology, Tsuyama, Japan
Yasuhiro MATSUNAGA
Anan National College of Technology, Anan, Japan

ABSTRACT

The present paper discusses thermal shock problems in transversely isotropic cylinders containing a penny-shaped crack or an external crack. Numerical calculations of the stress intensity factors are carried out for a transversely isotropic graphite which is widely used to a structural material in a reactor. The maximum stress intensity factors with respect to a time variable are approximated by a function of Biot's number and crack length.

1 INTRODUCTION

When structural materials in a reactor are subjected to rapid cooling or rapid heating, the materials are subjected to the thermal shock. If there are cracks in such materials, the materials may be fracture due to the stress concentrations at the crack tips. By the way, transversely isotropic materials such as a graphite, a cadmium and a beryllium are widely used to structures in a reactor. For that, it is very important to estimate the stress concentrations at the crack tips in the transversely isotropic materials containing various shaped cracks subjected to the thermal shock.

A considerable effort has been devoted to calculations of thermal stresses associated with various types of crack. Most of these, however, are concerned with isotropic solids. Thermoelastic crack problems in anisotropic solids have been treated only in a limited number of papers (Noda and Ashida 1987). The thermal shock problem in an anisotropic cylinder containing a crack has not been investigated so far.

The present paper discusses the thermal shock problems in two types of the transversely isotropic cylinder containing a penny-shaped crack or an external crack. It is assumed that the thermal disturbance due to the crack is neglected in the analysis of the temperature field, because the thermal shock is short lived. Numerical calculations of the stress intensity factors are carried out for a graphite and compared with those derived under isotropic conditions. The maximum stress intensity factors with respect to a time variable are approximated by a function of Biot's number and crack length.

2 ANALYSIS

2.1 Temperature field

Let consider the heat conduction problem for transversely isotropic infinite cylinders of radius a containing a penny-shaped crack of radius b or an external crack of crack length b. It is assumed that the thermal disturbance due to the crack is neglected in the analysis of temperature field, because thermal shock is short lived.

The governing equation for transient heat conduction is given by

$$\Delta_1 T = T_{,t}/\kappa \tag{1}$$

where $\Delta_1 = \partial^2/\partial r^2 + r^{-1}\partial/\partial r$, T is the temperature, $T_{,t} = \partial T/\partial t$, t is the time variable and κ is the thermal diffusivity.

The initial and boundary conditions for temperature field are expressed by

$$T = T_0 \quad \text{at } t=0 \tag{2}$$

$$T_{,r} = -h(T-T_c) \quad \text{on } r=a \tag{3}$$

where h is the relative heat transfer coefficient on the cylindrical surface.

Applying the Laplace transform with respect to the time variable, the solution of Eq.(1) which satisfies Eqs.(2) and (3) is expressed by

$$T = T_0 + (T_c - T_0)\{1 - \sum_{m=1}^{\infty} T_m J_0(\beta_m r)\} \tag{4}$$

where

$$T_m = 2h \cdot \exp(-\kappa\beta_m^2 t)/a(\beta_m^2 + h^2)J_0(\beta_m a), \quad \beta J_1(\beta a) - hJ_0(\beta a) = 0. \tag{5}$$

2.2 Thermal stresses

Let consider a transient thermoelastic problems for a transversely isotropic infinite cylinders containing a penny-shaped crack or an external crack. The convective heating for the penny-shaped crack and the convective cooling for the external crack act on the lateral surfaces of cylinders, so the crack surfaces open. The thermal stress field can be analyzed by means of the transversely isotropic potential function method (Takeuti and Noda 1978).

The stress-strain relations are expressed by

$$\left.\begin{aligned} &\sigma_{rr} = c_{11}\varepsilon_{rr} + c_{12}\varepsilon_{\theta\theta} + c_{13}\varepsilon_{zz} - \bar{\beta}_1(T-T_0), \quad \sigma_{\theta\theta} = c_{12}\varepsilon_{rr} + c_{11}\varepsilon_{\theta\theta} + c_{13}\varepsilon_{zz} - \bar{\beta}_1(T-T_0), \\ &\sigma_{zz} = c_{13}\varepsilon_{rr} + c_{13}\varepsilon_{\theta\theta} + c_{33}\varepsilon_{zz} - \bar{\beta}_3(T-T_0), \quad \sigma_{rz} = c_{44}\varepsilon_{rz}. \end{aligned}\right\} \tag{6}$$

We introduce the potential functions χ_i and ϕ_i which relate to the displacements as follows:

$$u_r = (\chi_1 + \phi_1 + \phi_2)_{,r}, \quad u_z = (\chi_2 + k_1\phi_1 + k_2\phi_2)_{,z}. \tag{7}$$

The potential functions must satisfy the following equations.

$$\left.\begin{aligned} &c_{11}\Delta_1\chi_1 + c_{44}\chi_{1,zz} + (c_{13}+c_{44})\chi_{2,zz} = \bar{\beta}_1(T-T_0), \\ &(c_{13}+c_{44})\Delta_1\chi_1 + c_{44}\Delta_1\chi_2 + c_{33}\chi_{2,zz} = \bar{\beta}_3(T-T_0) \end{aligned}\right\} \tag{8}$$

$$\Delta_1\phi_i + \mu_i\phi_{i,zz} = 0 \quad (i=1,2) \tag{9}$$

where

$$c_{11}c_{44}\mu^2 + (2c_{13}c_{44} + c_{13}^2 - c_{11}c_{33})\mu + c_{33}c_{44} = 0, \quad k_i = (c_{11}\mu_i - c_{44})/(c_{13}+c_{44}) \quad (i=1,2).$$

We assume the admissible solutions for the potential functions in the form:

$$\chi_i = (T_c - T_0)A_i\{r^2/4 + \sum_{m=1}^{\infty} T_m J_0(\beta_m r)/\beta_m^2\} \quad (i=1,2) \tag{10}$$

$$\phi_i = -(T_c - T_0)[F_i(r^2/4 - z^2/2\mu_i) + \sum_{m=1}^{\infty} D_{im} J_0(\beta_m r)\exp(-\beta_m z/\sqrt{\mu_i})/\beta_m^2 + \int_0^{\infty} p^{-2} E_{ip} I_0(p\sqrt{\mu_i}\, r)\cos(pz)\,dp] \quad (i=1,2) \tag{11}$$

where A_i, F_i, D_{im} and E_{ip} are the unknown coefficients. Substituting Eqs.(4) and (10) into Eqs.(8), A_1 and A_2 can be determined.

Substituting Eqs.(4), (10) and (11) into Eqs.(7) and (6), we can derive the displacements and stresses.

$$u_z = (T_c - T_0)\sum_{i=2}^{\infty}[k_i F_i z/\mu_i + \sum_{m=1}^{\infty} k_i D_{im} J_0(\beta_m r)\exp(-\beta_m z/\sqrt{\mu_i})/\beta_m\sqrt{\mu_i} + \int_0^{\infty} p^{-1} k_i E_{ip} I_0(p\sqrt{\mu_i}\, r)\sin(pz)\,dp \tag{12}$$

$$\sigma_{zz} = -(T_c - T_0)[\sum_{i=2}^{\infty}(c_{13}\mu_i - c_{33}k_i)[F_i/\mu_i - \sum_{m=1}^{\infty} D_{im} J_0(\beta_m r)\exp(-\beta_m z/\sqrt{\mu_i})/\mu_i + \int_0^{\infty} E_{ip} I_0(p\sqrt{\mu_i}\, r)\cos(pz)\,dp] - (c_{13}A_1 - \bar{\beta}_3)\{1 - \sum_{m=1}^{\infty} T_m J_0(\beta_m r)\}] \tag{13}$$

The traction free boundary conditions are given by

$$\int_0^a \sigma_{zz}\, r\,dr = 0 \quad \text{at } z \to \infty \tag{14}$$

$$\sigma_{rr}=\sigma_{zr}=0 \quad \text{on } r=a \tag{15}$$

$$\sigma_{rz}=0 \quad \text{on } z=0 \tag{16}$$

$$\left.\begin{array}{l}\sigma_{zz}=0 \ (0\leqq r<b), \quad u_z=0 \ (b\leqq r\leqq a) \quad \text{on } z=0 \quad \text{(penny-shaped crack)} \\ u_z=0 \ (0\leqq r\leqq c), \quad \sigma_{zz}=0 \ (c<r\leqq a) \quad \text{on } z=0 \quad \text{(external crack)}\end{array}\right\} \tag{17}$$

where $c=a-b$.

In order to solve Eqs.(15)-(17), we apply the Fourier integrals of $\sin(pz)$ and $\cos(pz)$ and Bessel series of $J_0(\beta_m r)$. F_1 and F_2 can be determined from Eq.(14) and the constant term of $[\sigma_{rr}]_{r=a}$. The other unknown coefficients are determined by means of the method of successive approximation. The solution only satisfied Eqs.(15) is approximation for $(2j)$-th times and the solution only satisfied Eqs.(16) and (17) is approximation for $(2j+1)$-th times. We can obtain the following equations from Eqs.(15) and (16).

$$E_{ip}^{2j}=\sum_{m=1}^{\infty}\{\Psi_{i1}D_{1m}^{2j+1}+\Psi_{i2}D_{2m}^{2j+1}\} \quad (i=1,2), \quad D_{2m}^{2j+1}=\Omega_1 D_{1m}^{2j+1} \quad (j=0,1,2,\cdots) \tag{18}$$

where Ψ_{i1}, Ψ_{i2} and Ω_i are the known coefficients. Eqs.(17) reduce to the following dual series equation.

$$\left.\begin{array}{l}\displaystyle\sum_{m=1}^{\infty}G_m^{2j+1}J_0(\beta_m r)=0 \quad (j=0,1,2,\cdots) \quad \begin{array}{l}(0\leqq r<b, \text{ penny-shaped crack}) \\ (c<r\leqq a, \text{ external crack})\end{array} \\ \displaystyle\sum_{m=1}^{\infty}\Phi_m G_m^{2j+1}J_0(\beta_m r)=\sum_{m=1}^{\infty}\Phi_m[(1-\delta_{j0})\int_0^{\infty}\{\Gamma_{1mp}E_{1p}^{2j}+\Gamma_{2mp}E_{2p}^{2j}\}dp+\delta_{j0}A]J_0(\beta_m r) \\ \qquad (j=0,1,2,\cdots) \quad \begin{array}{l}(b\leqq r\leqq a, \text{ penny-shaped crack}) \\ (0\leqq r\leqq c, \text{ external crack})\end{array}\end{array}\right\} \tag{19}$$

where

$$G_m^{2j+1}=\Omega_2 D_{1m}^{2j+1}+(1-\delta_{j0})\int_0^{\infty}\{\Gamma_{1mp}E_{1p}^{2j}+\Gamma_{2mp}E_{2p}^{2j}\}dp+\delta_{j0}A. \tag{20}$$

and Ω_2, Φ_m, Γ_{1mp}, Γ_{2mp} and A are the known coefficients. In order to solve the dual series equation, we introduce the following functions which satisfy the first of Eqs.(19).

$$\sum_{m=1}^{\infty}G_m^{2j+1}J_0(\beta_m r)=f(r)\sum_{k=0}^{\infty}x_k^{2j+1}\cos(k\theta) \tag{21}$$

where x_k are the unknown coefficients, and

$$\left.\begin{array}{l}r^2=r_c^2+r_w^2-2r_c r_w\cos\theta, \quad r_c=(a+b)/2, \quad r_w=(a-b)/2 \\ f(r)=H(r-b)/\sqrt{r^2-b^2}\end{array}\right\} \text{(penny-shaped crack)}$$

$\sin\theta=r/c$, $f(r)=H(c-r)/\sqrt{c^2-r^2}$ (external crack).

Applying the inverse Hankel transform to Eq.(21), G_m are expressed by

$$G_m^{2j+1}=\sum_{k=0}^{\infty}L_{mk}x_k^{2j+1} \tag{22}$$

where L_{mk} are the known coefficients. Substituting Eq.(22) into the second of Eqs.(19) and applying the Neumann series, we get the following infinite system of simultaneous algebraic equations which determines the unknown coefficients.

$$\sum_{k=0}^{\infty}x_k^{2j+1}\sum_{m=1}^{\infty}\Phi_m L_{mk}Z_{im}=\sum_{m=1}^{\infty}\Phi_m[(1-\delta_{j0})\int_0^{\infty}\{\Gamma_{1mp}E_{1p}^{2j}+\Gamma_{2mp}E_{2p}^{2j}\}dp+\delta_{j0}A]Z_{im}, \quad (i=0,1,2,\cdots) \tag{23}$$

where

$$\left.\begin{array}{l}Z_{im}=J_i(\beta_m r_c)J_i(\beta_m r_w)-J_{i+2}(\beta_m r_c)J_{i+2}(\beta_m r_w) \quad \text{(penny-shaped crack)} \\ Z_{im}=J_i^2(\beta_m c/2)-J_{i+2}^2(\beta_m c/2) \quad \text{(external crack)}.\end{array}\right\} \tag{24}$$

The stress intensity factors are given by

$$\left.\begin{array}{l}K_I=-(T_c-T_0)\sqrt{\pi/b}\displaystyle\sum_{k=0}^{\infty}\sum_{j=0}^{\infty}x_k^{2j+1} \quad \text{(penny-shaped crack)} \\ \quad=(T_0-T_c)\sqrt{\pi/c}\displaystyle\sum_{k=0}^{\infty}(-1)^k\sum_{j=0}^{\infty}x_k^{2j+1} \quad \text{(external crack)}.\end{array}\right\} \tag{25}$$

3 NUMERICAL EXAMPLES

For convenience in numerical calculations, the following dimensionless

quantities are introduced:

$$t'=\kappa t/a^2,\quad B_i=ah,\quad \gamma=b/a,\quad E=E_z/E_r,\quad G=G_{rz}/E_r,\quad \alpha=\alpha_z/\alpha_r,$$

$$\hat{K}_I=K_I/\sqrt{b}\alpha_r E_r(T_c-T_\infty)\quad\text{(penny-shaped crack)}$$

$$=K_I/\sqrt{b}\alpha_r E_r(T_\infty-T_c)\quad\text{(external crack)}$$

where E_r, E_z and G_{rz} are the moduli of elasticity, α_r and α_z are the coefficients of liner thermal expansion, t' is Fourier's number, B_i is Biot's number.

The material constants are taken as for a graphite which possesses transverse isotropy

$$E_r=10.4\ \text{GPa},\quad E_z=11.8\ \text{GPa},\quad G_{rz}=4.14\ \text{GPa},\quad \nu_{r\theta}=\nu_{rz}=0.11,$$
$$\alpha_r=3.9\times10^{-6}\ \text{K}^{-1},\quad \alpha_z=3.5\times10^{-6}\ \text{K}^{-1}$$

and for isotropic conditions

$$E=\alpha=1,\quad G=E/2(1+\nu_{rz}),\quad \nu_{r\theta}=\nu_{rz}=0.11$$

where $\nu_{r\theta}$ and ν_{rz} are the Poisson's ratios.

3.1 Penny-shaped crack

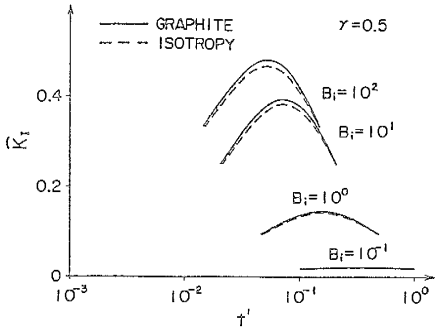

Fig.1 Time variation of $\hat{K}_I$

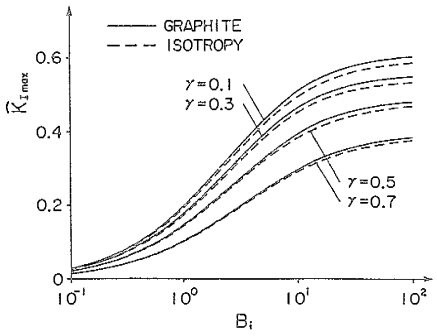

Fig.2 Relation between $\hat{K}_{I\max}$ and B_i

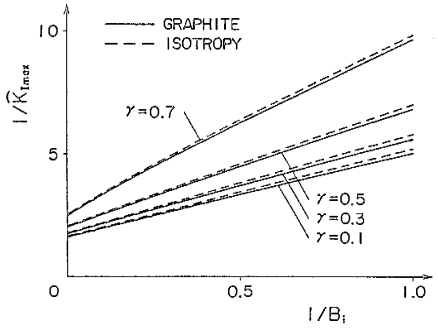

Fig.3 Relation between $1/\hat{K}_{I\max}$ and $1/B_i$

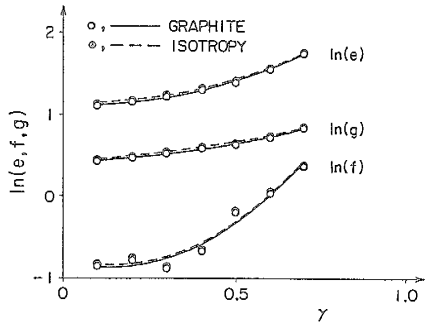

Fig.4 Values of coefficients e, f and g

Fig.1 illustrates the time variation of stress intensity factor. The stress intensity factor has the maximum value with respect to Fourier's number and increases according with Biot's number. The stress intensity factor for a graphite is somewhat lager than that derived under isotropic conditions. Fig.2 illustrates the relation between the maximum stress intensity factor and Biot's number. This figure shows that the maximum stress intensity factor increases with decreasing crack length. Fig.3 illustrates the relation between the inverse maximum stress intensity factor and inverse Biot's number. The inverse maximum stress intensity factor for small Biot's number can be

expressed by a linear equation of inverse Biot's number, but that for large Biot's number deviates from the linear equation. Therefore, we propose the following equation.

$$1/\hat{K}_{I\,max}=e/B_i+f/\sqrt{B_i}+g \quad (0.1\leqq B_i\leqq 100) \tag{26}$$

The coefficients e, f and g can be determined by the method of least squares. The calculated values are plotted in Fig.4. The coefficients e, f and g can be expressed as following equations by means of the method of least squares.

graphite $(0.1\leqq\gamma\leqq 0.7)$

$\ln(e)=1.460\gamma^2-0.131\gamma+1.126,$

$\ln(f)=4.224\gamma^2-1.229\gamma-0.779,$

$\ln(g)=0.610\gamma^2+0.183\gamma+0.415$

isotropic conditions $(0.1\leqq\gamma\leqq 0.7)$

$\ln(e)=1.419\gamma^2-0.115\gamma+1.155,$

$\ln(f)=4.174\gamma^2-1.208\gamma-0.750,$

$\ln(g)=0.580\gamma^2+0.193\gamma+0.445$

The relative errors between the maximum stress intensity factor calculated from Eq.(25) and that calculated from Eq.(26) are shown in Table 1. We consider that Eq.(26) gives a close approximation, because the errors are less than 2.6%. The errors for isotropic conditions are same as those for the graphite.

Table 1 Errors of approximation in Eq.(26) for graphite

γ	B_i 0.1	1	10	100
0.1	-0.9	-0.6	-1.9	1.9
0.2	0.8	1.1	-1.1	2.2
0.3	0.9	1.1	-1.3	2.6
0.4	0.4	0.8	-1.5	1.9
0.5	-1.0	0.1	-1.7	1.4
0.6	-0.8	-0.2	-1.5	1.6
0.7	0.8	0.4	-1.0	2.3

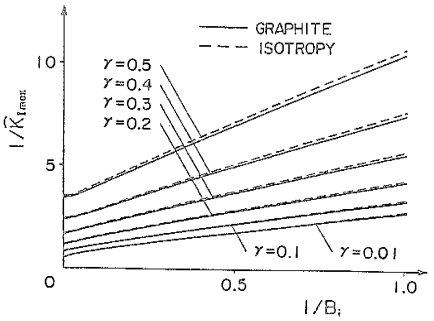

Fig.5 Relation between $1/\hat{K}_{I\,max}$ and $1/B_i$

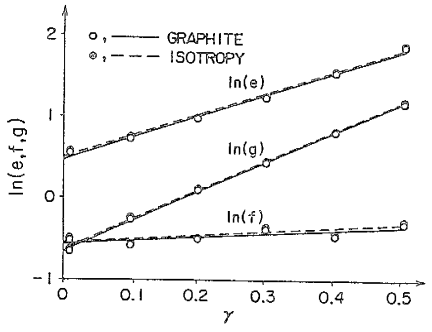

Fig.6 Values of coefficients e, f and g

Table 2 Errors of approximation in Eq.(26) for graphite

γ	B_i 0.1	1	10	100
0.01	5.0	3.9	0.8	-5.6
0.1	-1.1	-0.5	0.2	3.6
0.2	-3.3	-1.7	-0.4	4.3
0.3	-3.8	-2.0	-1.7	2.6
0.4	-1.0	-0.5	-3.0	1.3
0.5	4.8	4.1	-1.6	2.2

3.2 External crack

Fig.5 illustrates the relation between the inverse maximum stress intensity factor and inverse Biot's number. It is clear that the maximum stress intensity factor increases with decreasing crack length. We use Eq.(26) for approximation of the maximum stress intensity factor. The values of coefficients e, f and g can be determined by means of the method of least squares and are plotted in Fig.6. Furthermore, the coefficients e, f and g

can be expressed as following equations by use of the method of least squares.

graphite $(0.01 \leqq \gamma \leqq 0.5)$	isotropic conditions $(0.01 \leqq \gamma \leqq 0.5)$
$\ln(e)=2.720\gamma+0.458$,	$\ln(e)=2.716\gamma+0.483$,
$\ln(f)=0.445\gamma-0.579$,	$\ln(f)=0.485\gamma-0.558$,
$\ln(g)=3.649\gamma-0.634$	$\ln(g)=3.643\gamma-0.609$

The relative errors between the maximum stress intensity factor calculated from Eq.(25) and that calculated from Eq.(26) are shown in Table 2. The errors are less than 5.6%, so Eq.(26) gives a fairly good approximation. The errors for isotropic conditions are same as those for the graphite. Figs.7-9 illustrate the effects of anisotropies of the transversely isotropic material constants on the inverse maximum stress intensity factor, when only one among the material constants such as E, G, $\nu_{r\theta}$ and α possesses various anisotropies, while the others are kept equal to those of isotropic conditions.

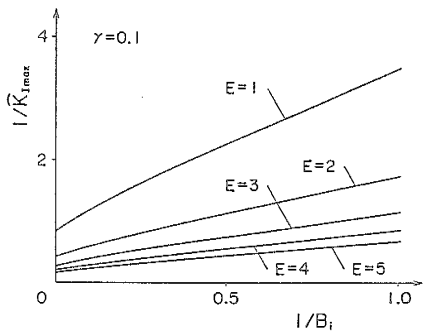

Fig.7 Effect of anisotropy of E on $1/\hat{K}_{I\max}$

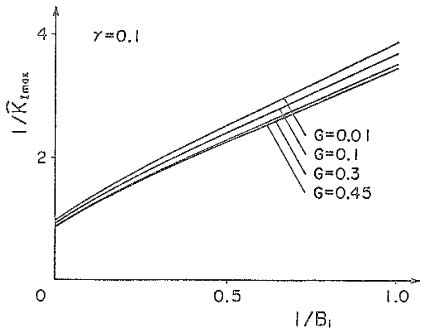

Fig.8 Effect of anisotropy of G on $1/\hat{K}_{I\max}$

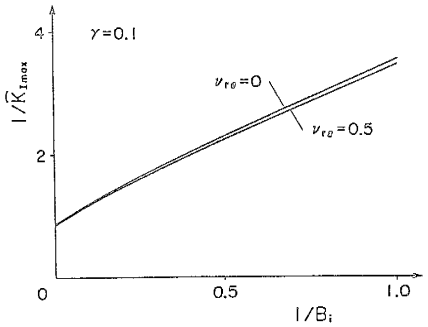

Fig.9 Effect of anisotropy of $\nu_{r\theta}$ on $1/\hat{K}_{I\max}$

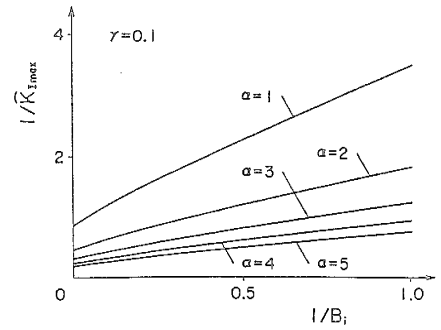

Fig.10 Effect of anisotropy of α on $1/\hat{K}_{I\max}$

REFERENCES

Noda, N and Ashida, F. (1987). Transient Thermoelastic Fields in a Transversely Isotropic Infinite Solid With a Penny-shaped Crack, Journal of Applied Mechanics, Vol.54, pp.854-860.

Noda, N. and Ashida, F. (1987). Stress Intensity Factor for Transient Thermal Stresses in a Transversely Isotropic Infinite Body with an External Crack, ACTA MECHANICA, Vol.66, pp.217-231.

Takeuti, Y. and Noda, N. (1978). A General Treatise on the Three-Dimensional Thermoelasticity of Curvilinear Aeorotropic Solids, Journal of Thermal Stresses, Vol.1, pp.25-39.